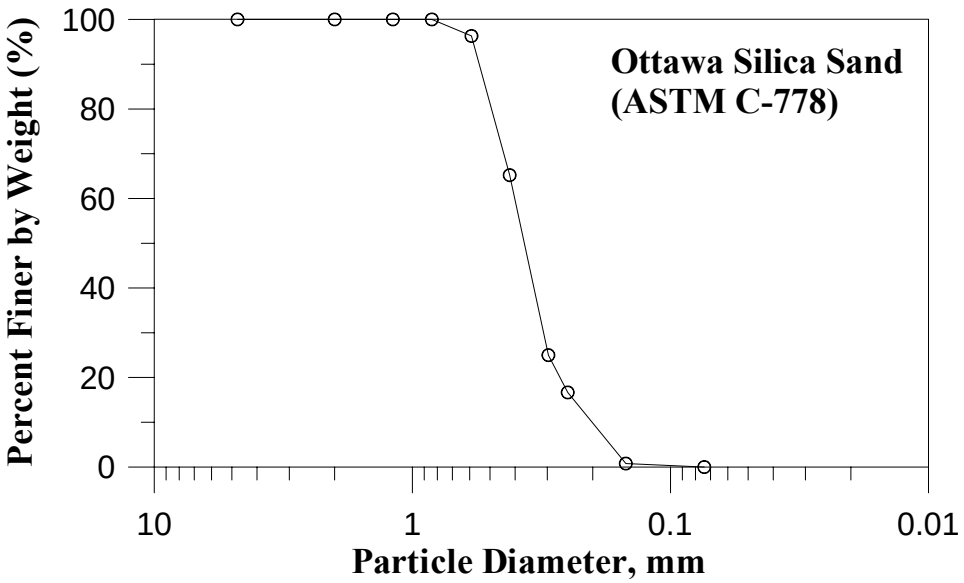

Fig. 5.1. Grain size distribution of Ottawa sand

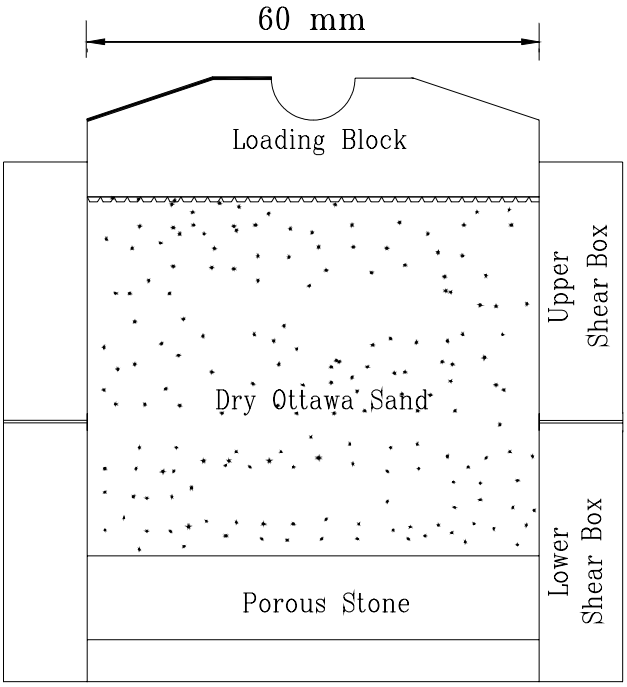

Unit : mm

Fig. 5.2. Shear box of direct shear test device
(after Wu, 1992)

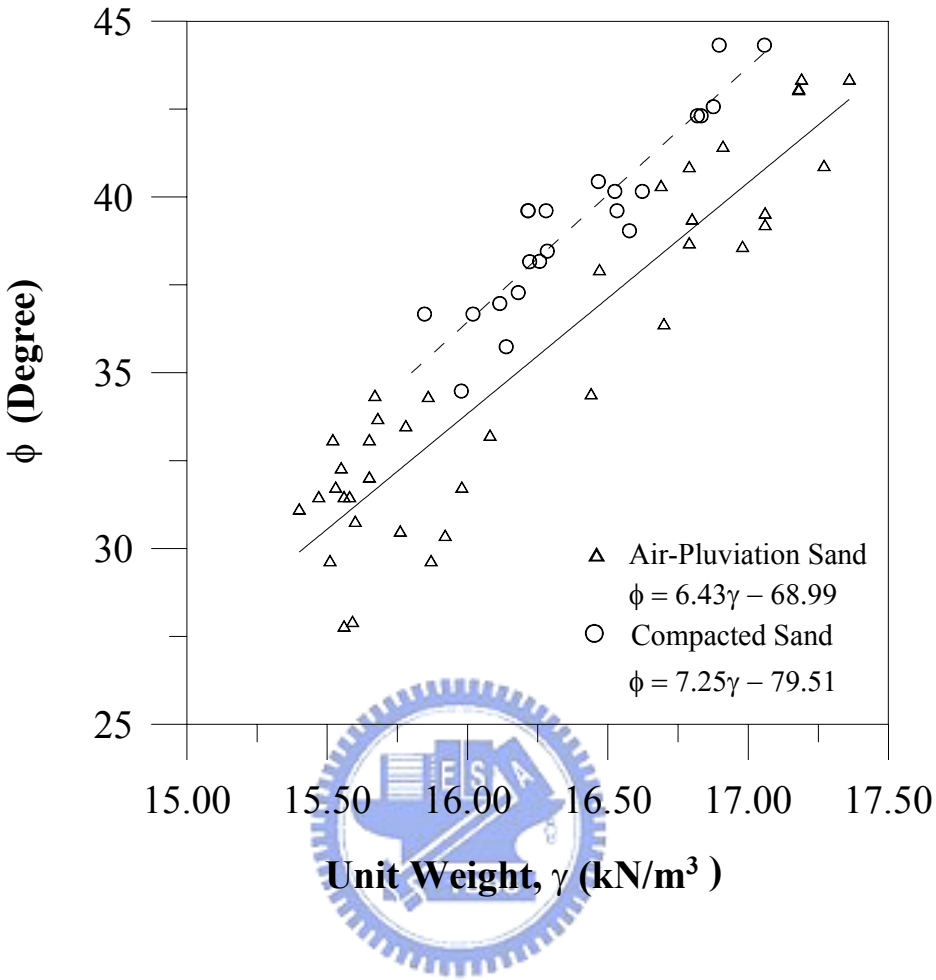

Fig. 5.3. Relationship between unit weight γ and internal friction angle (after Chang, 2000)

(a)

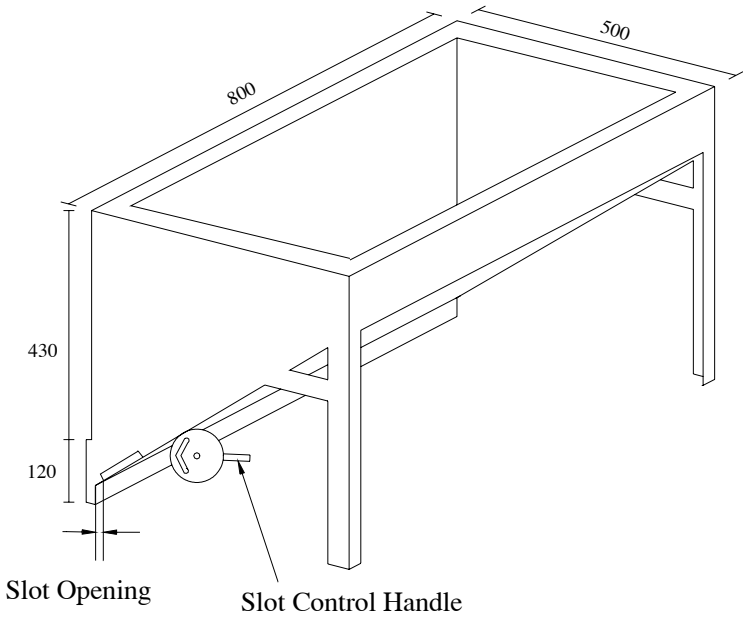

Unit:mm

(b)

Fig. 5.4. Soil hopper

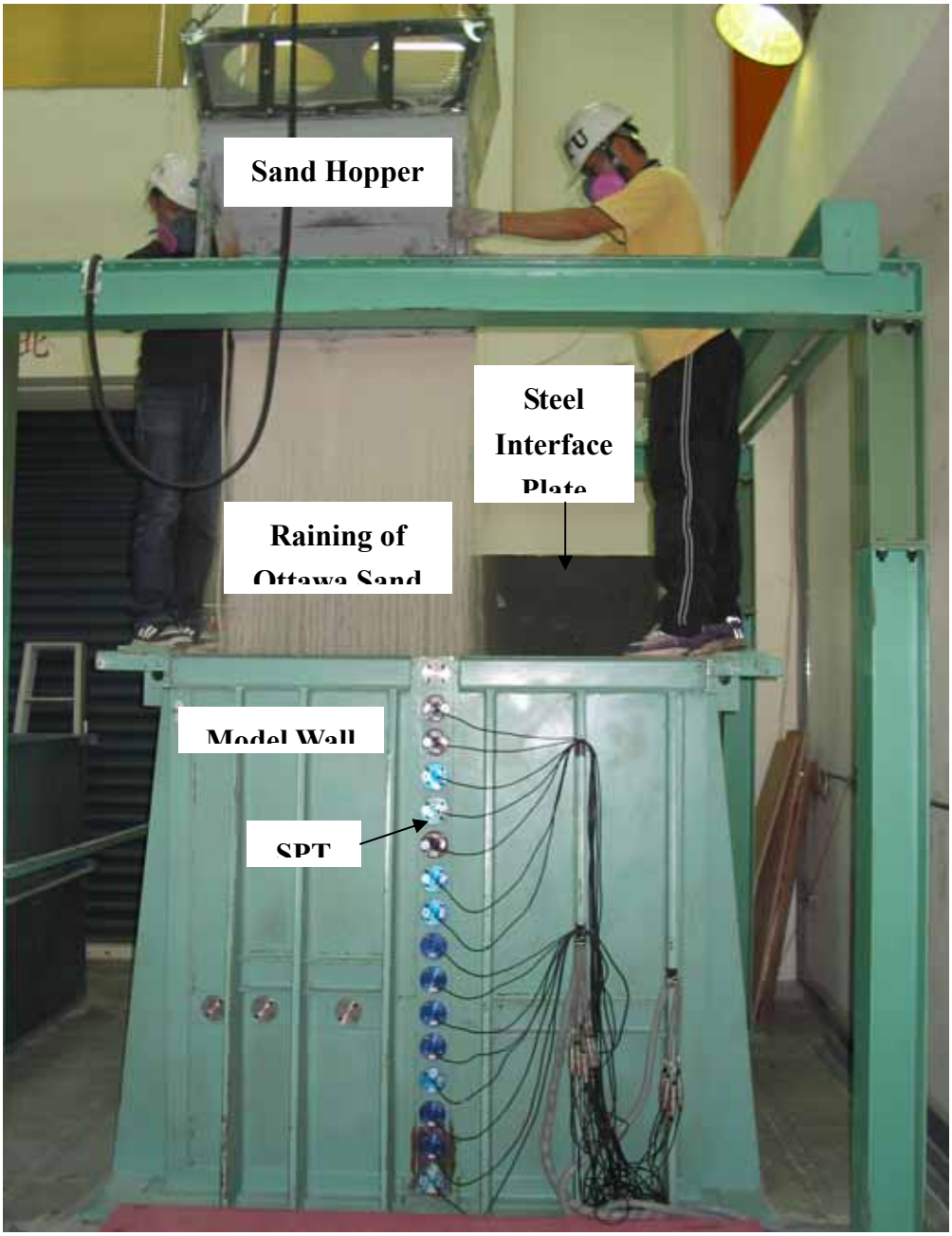

Fig. 5.5 Pluviation of the Ottawa sand into soil bin

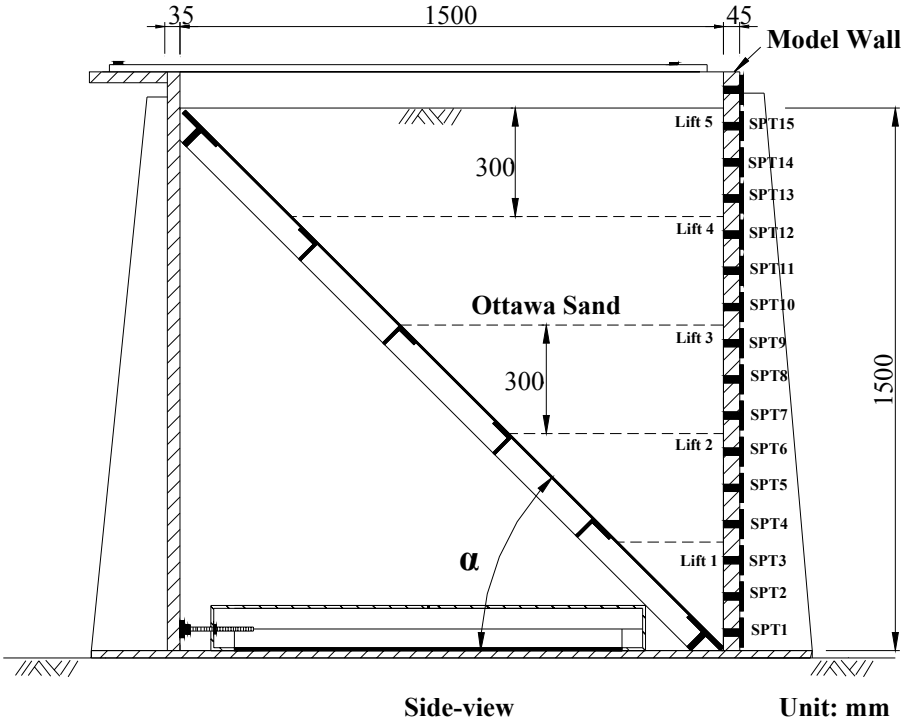

Fig. 5.6. Backfill compacted with square compactor in 5 lifts

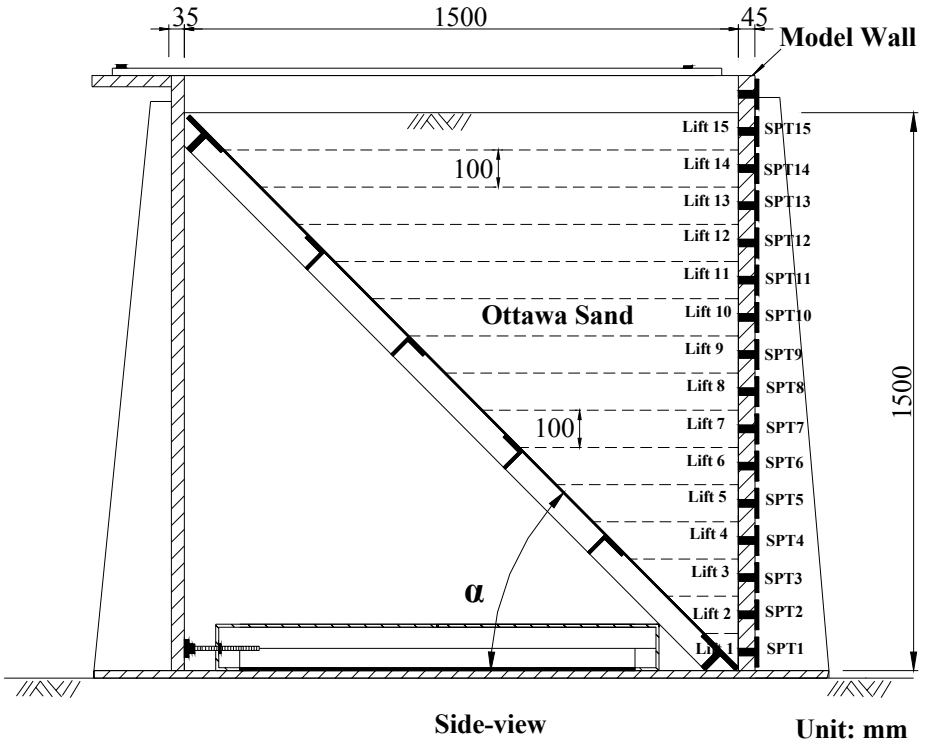

Fig. 5.7. Backfill compacted with strip compactor in 15 lifts

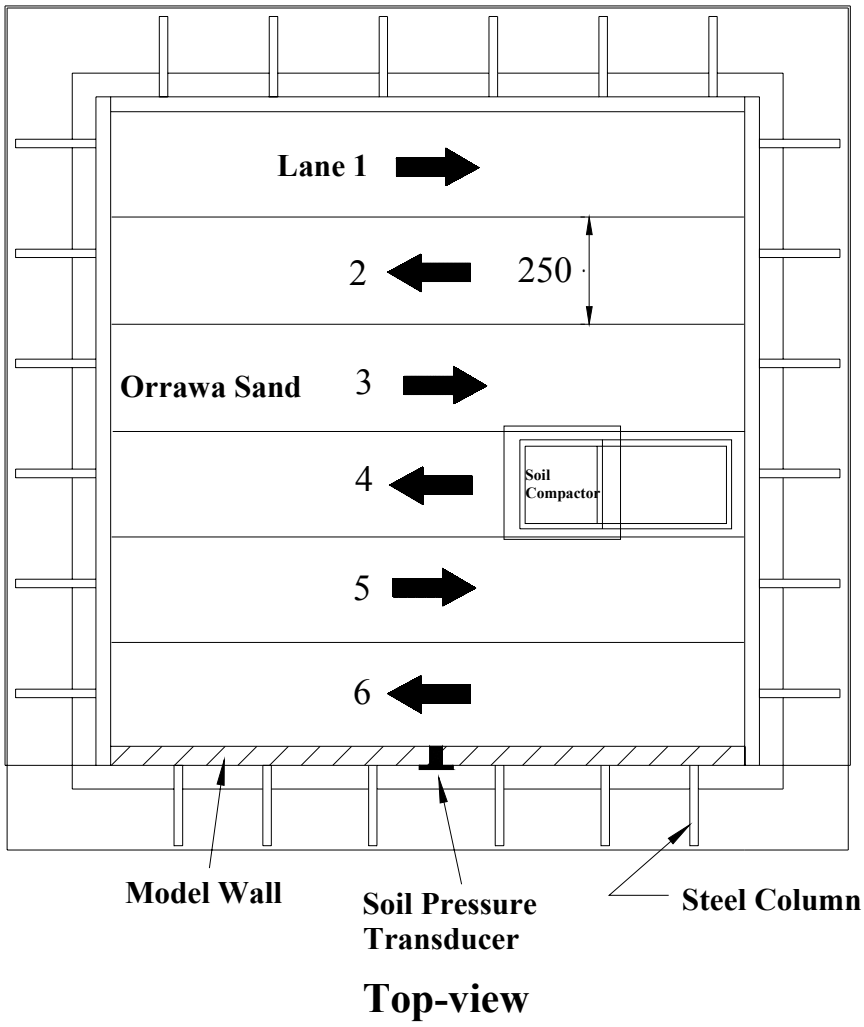

Fig. 5.8. Backfill compacted with square compactor in 6 lanes

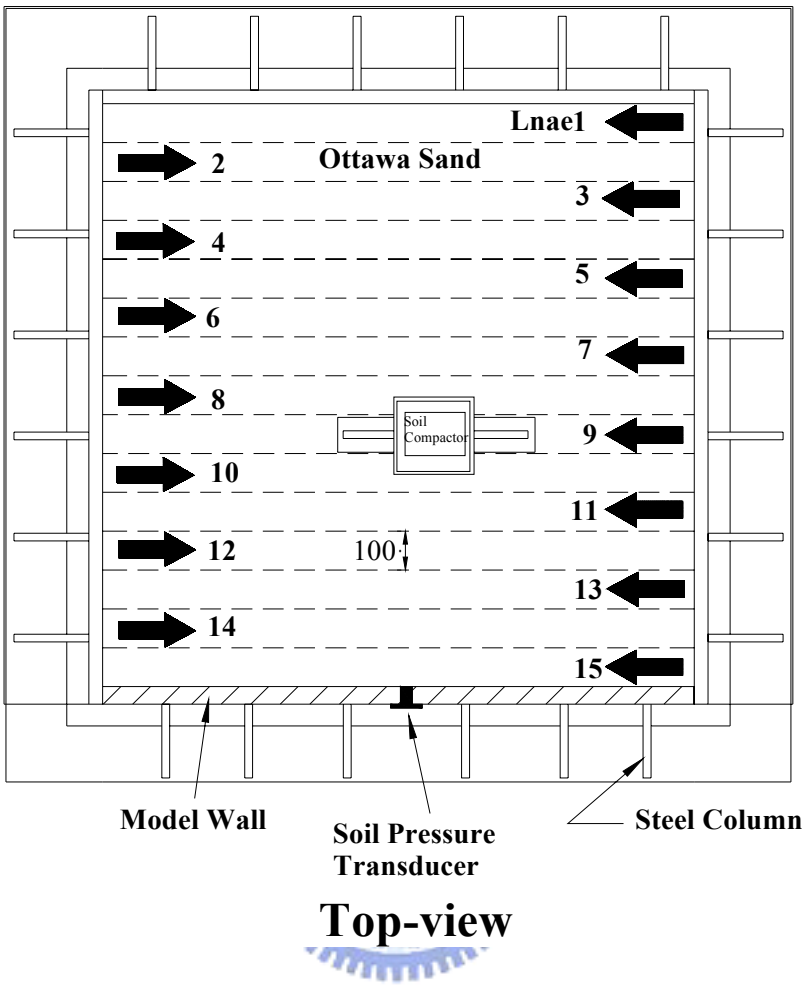

Fig. 5.9. Backfill compacted with strip compactor in 15 lances

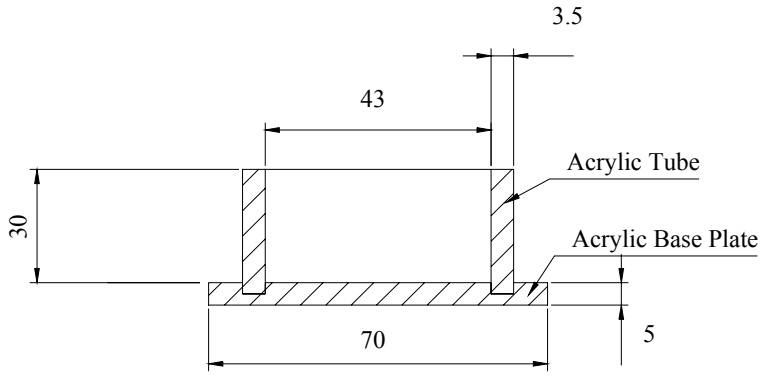

Side-view

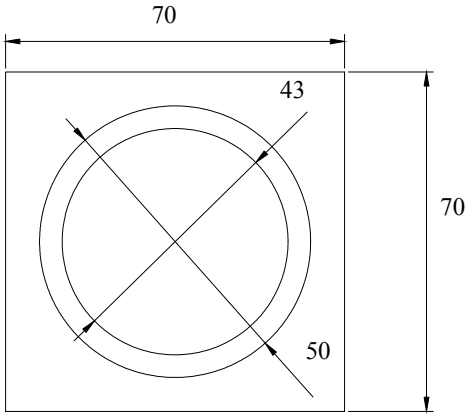

Top-view

unit : mm

Fig. 5.10. Soil-density control cup

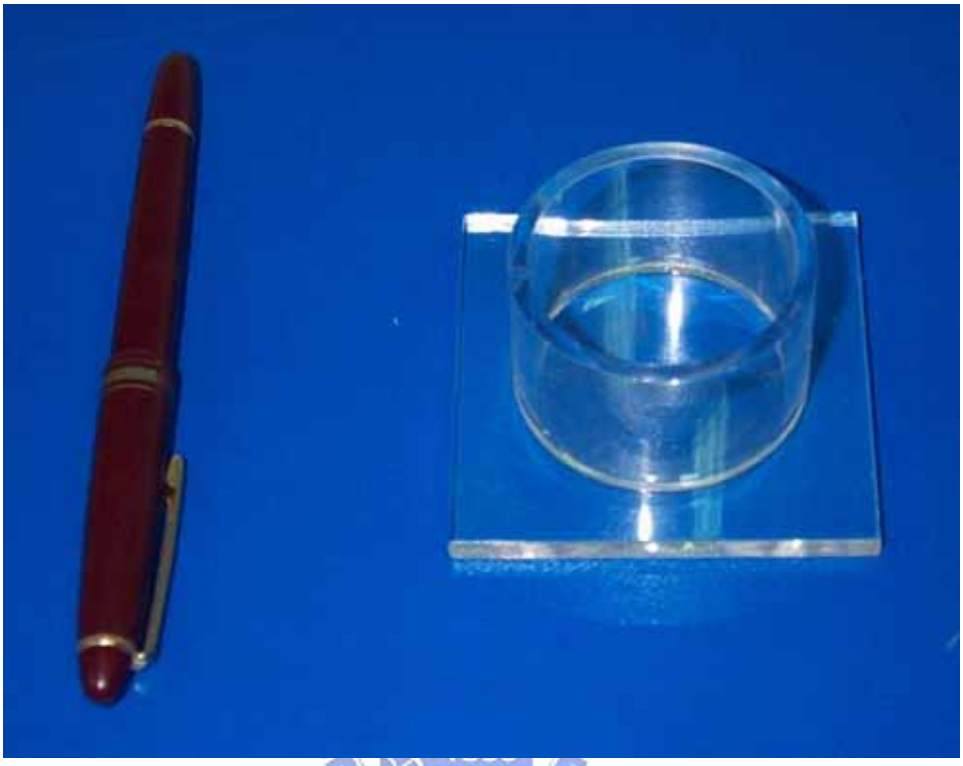

Fig. 5.11. Soil-density cup

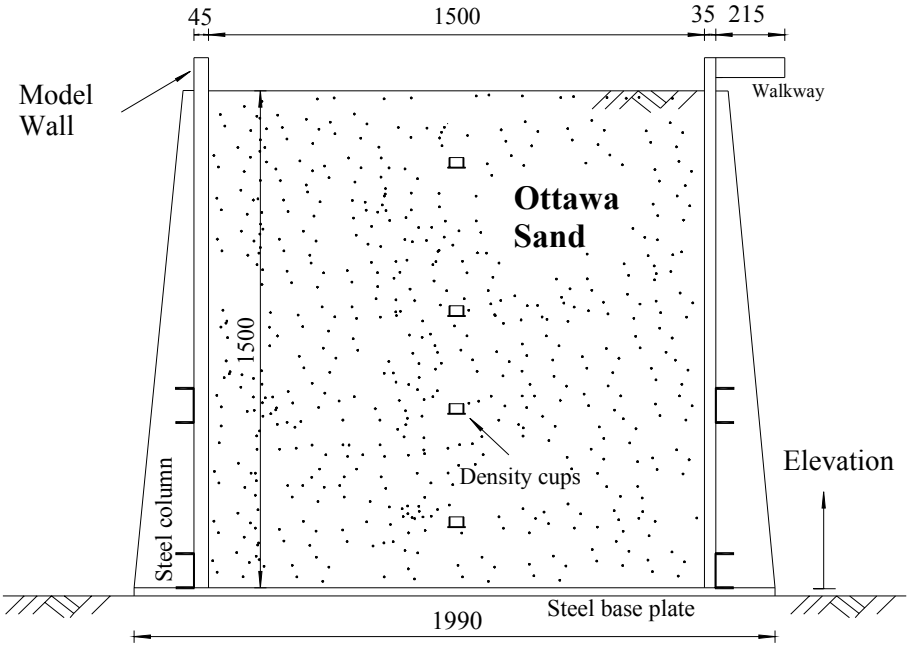

Unit : mm

Fig. 5.12. Soil density cups buried at the different elevations

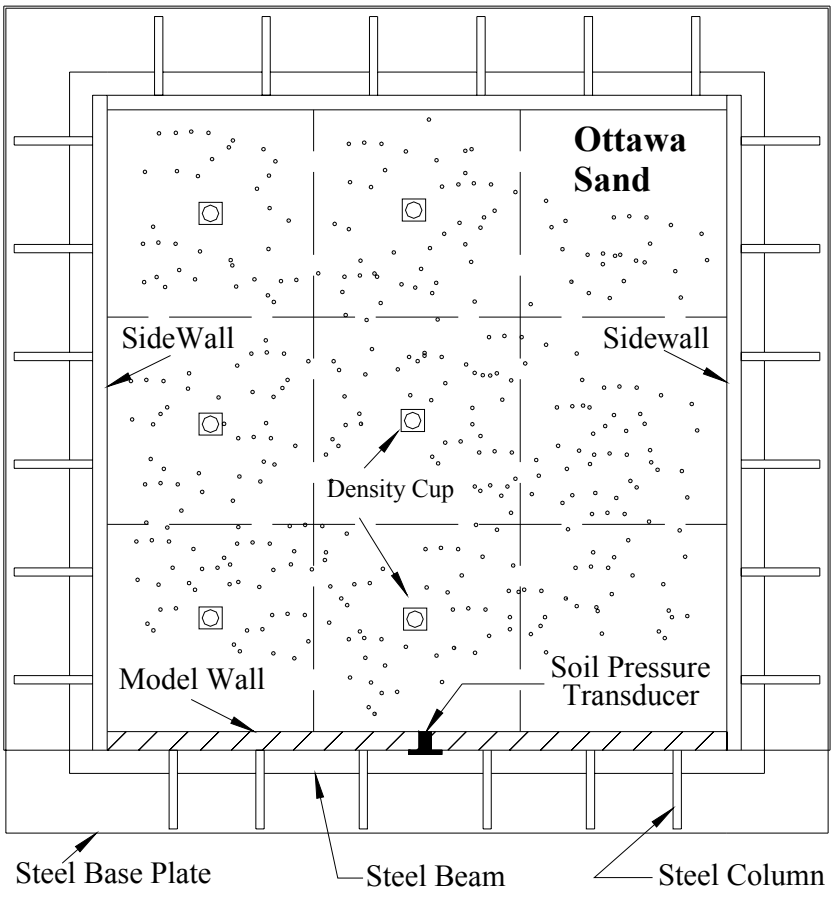

Fig. 5.13. Locations of soil density cups at same elevation

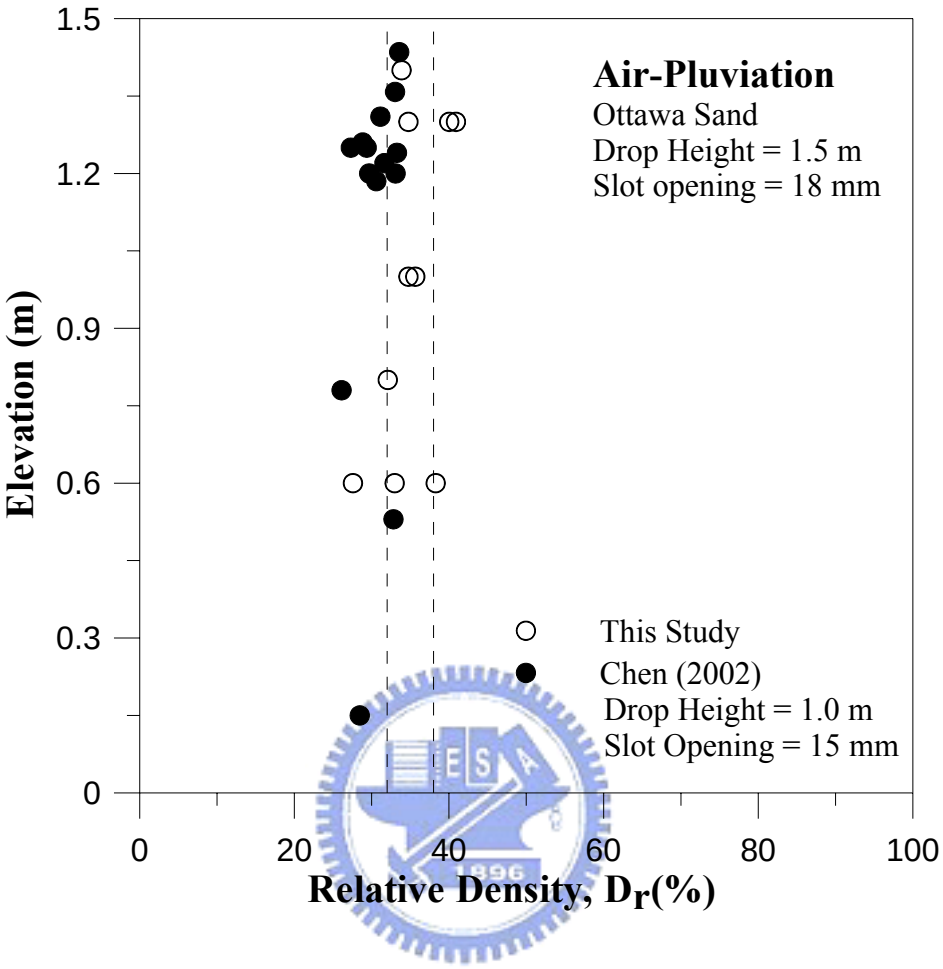

Fig. 5.14. Distribution of soil density for loose sand

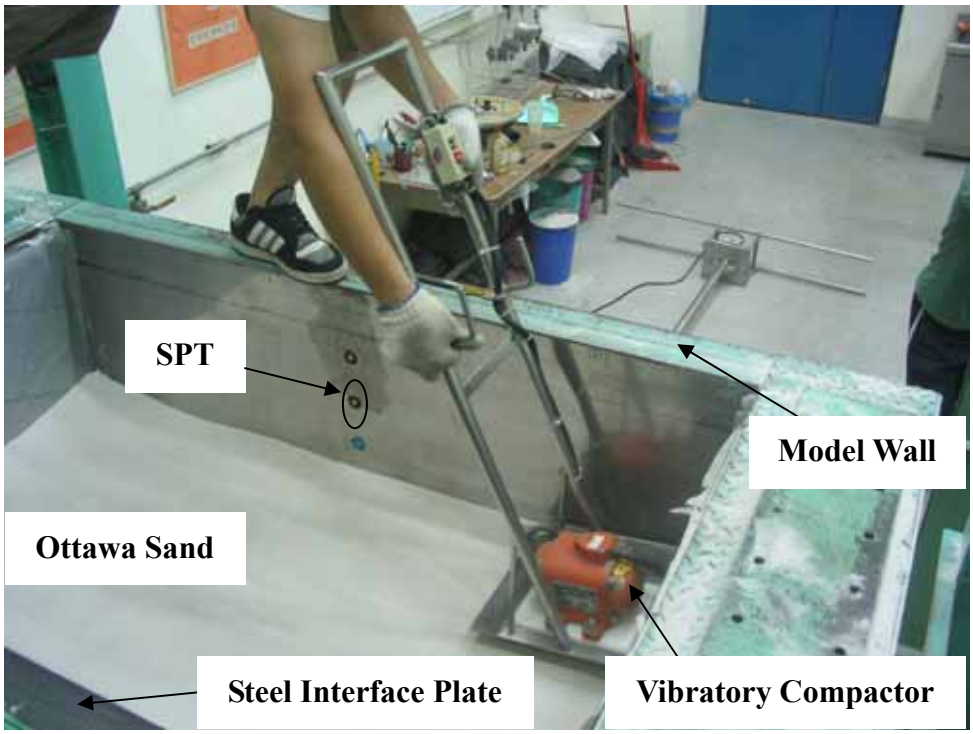

(a) Compaction at H = 1.2 m ($\alpha = 60^o$)

(b) Compaction at H = 1.2 m ($\alpha = 60^o$)

Fig. 5.15. Compaction of backfill with square compactor

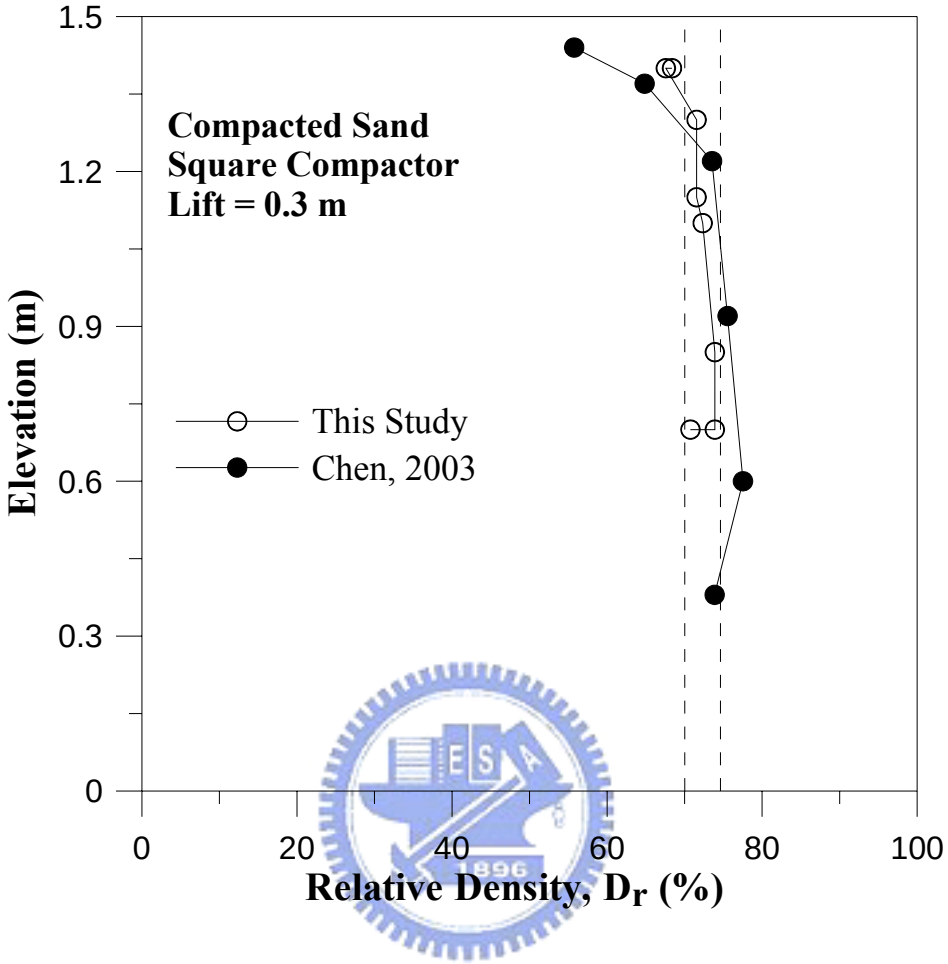

Fig. 5.16. Distribution of soil density compacted with square compactor

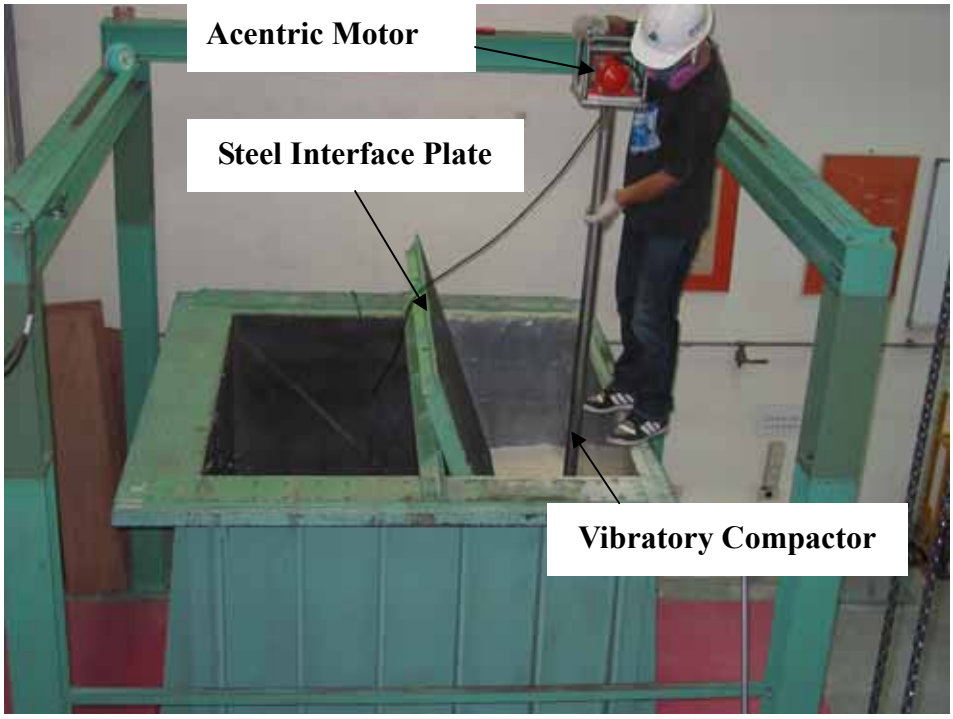

(a) Compaction at H = 1.1 m ($\alpha = 70^{o}$)

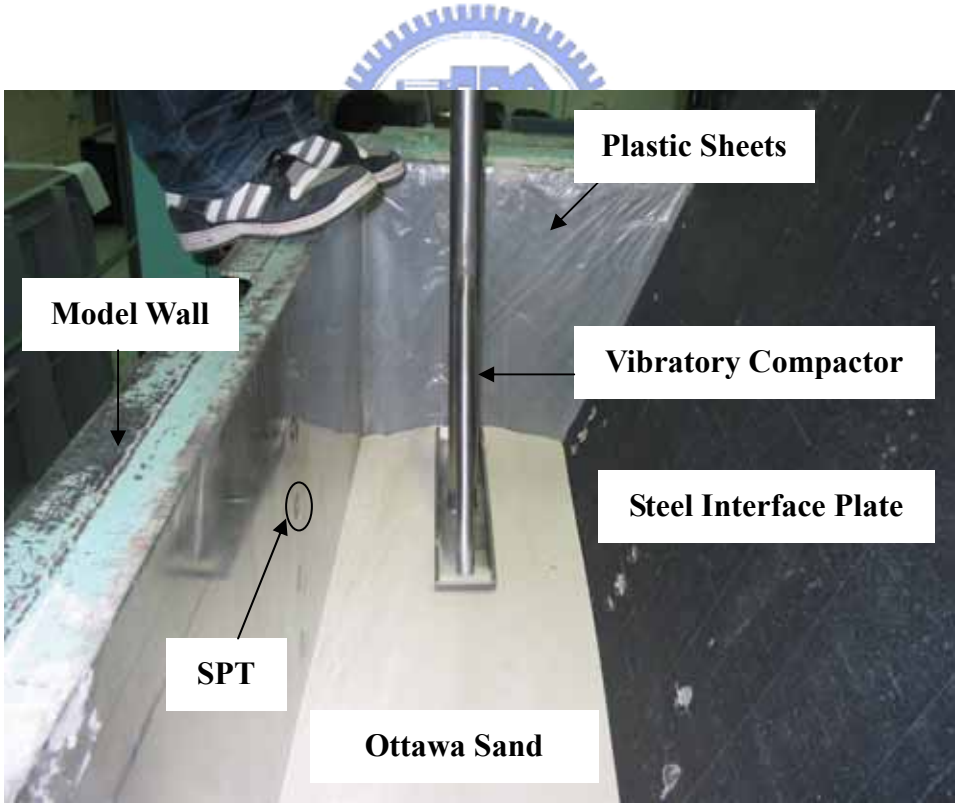

(b) Compaction at H = 1.1 m ($\alpha = 70^{o}$)

Fig. 5.17. Compaction of backfill with strip compactor

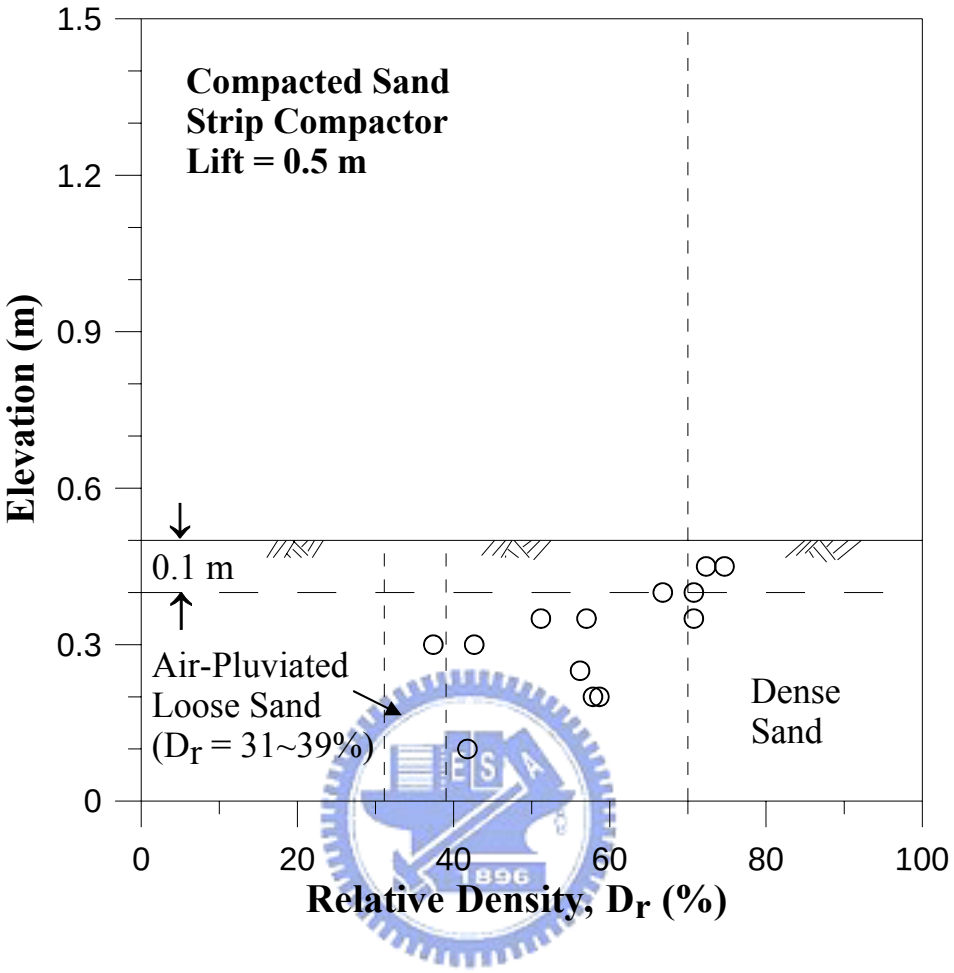

Fig. 5.18. Distribution of soil density compacted with strip compactor (Lift = 0.5 m)

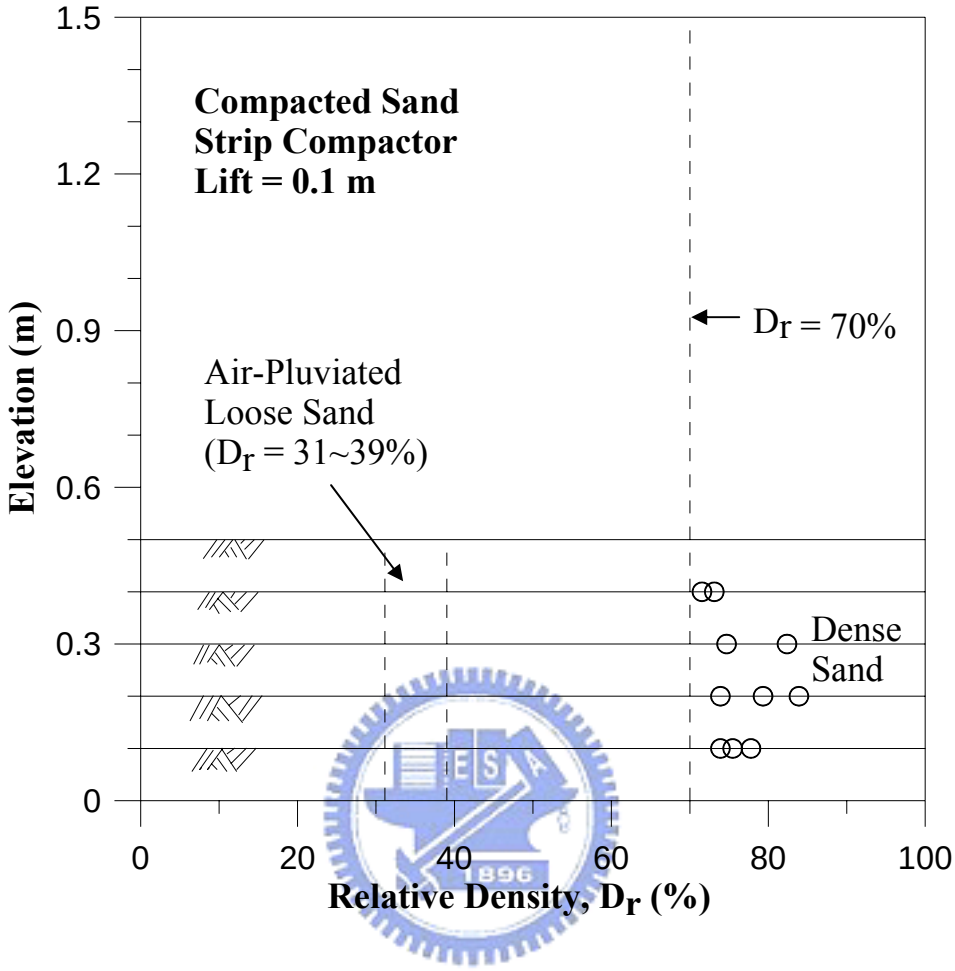

Fig. 5.19. Distribution of soil density compacted with strip compactor (Lift = 0.1 m)

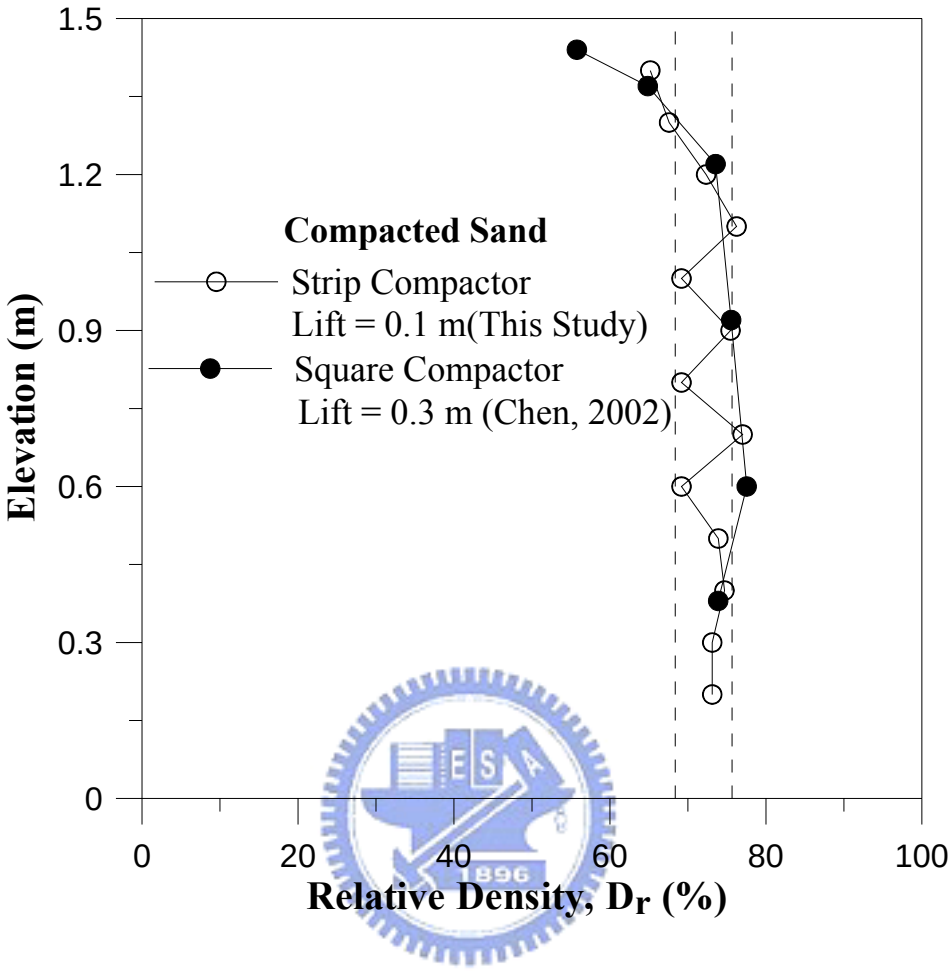

Fig. 5.20. Comparison of density distribution compacted with strip and square compactors

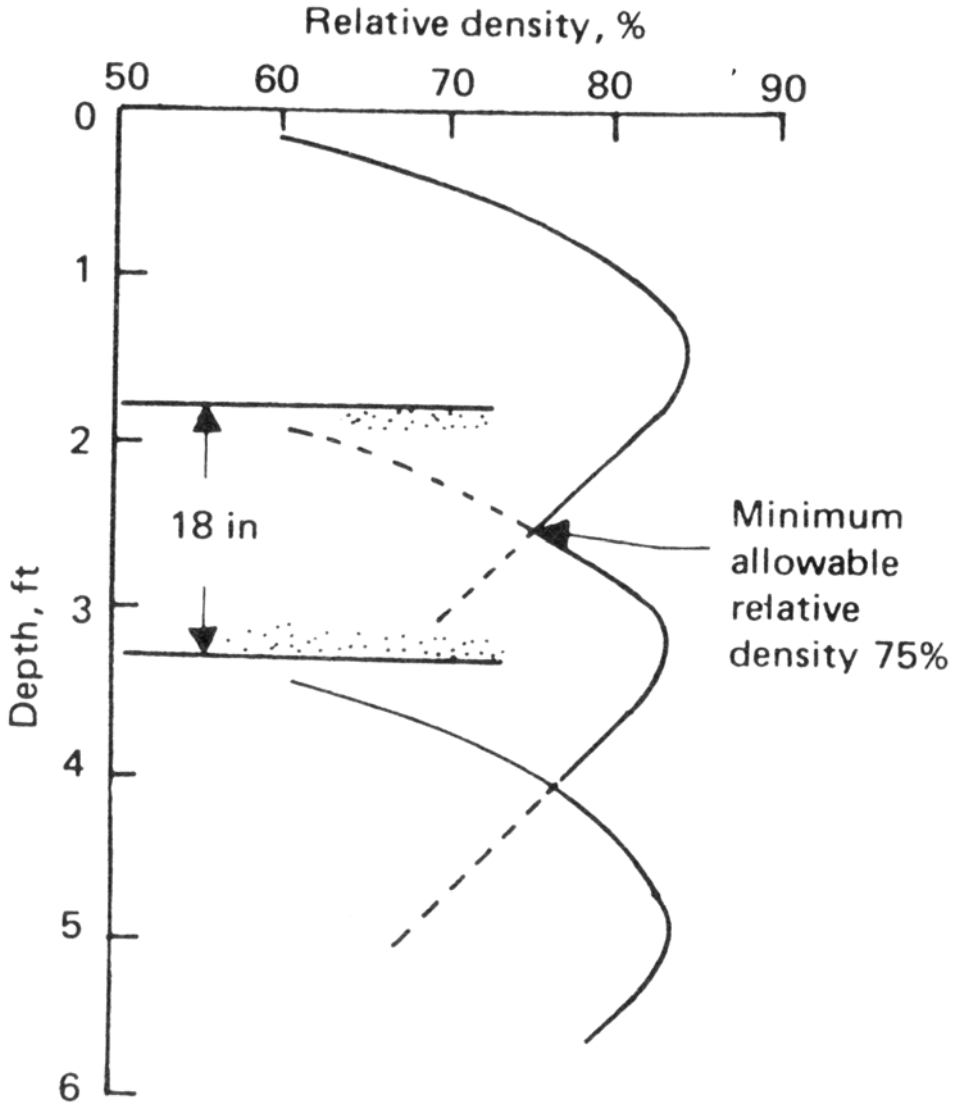

Fig. 5.21. Relative density vs. Depth relation for vibratory roller compaction (after D'Appolonia et al., 1969)

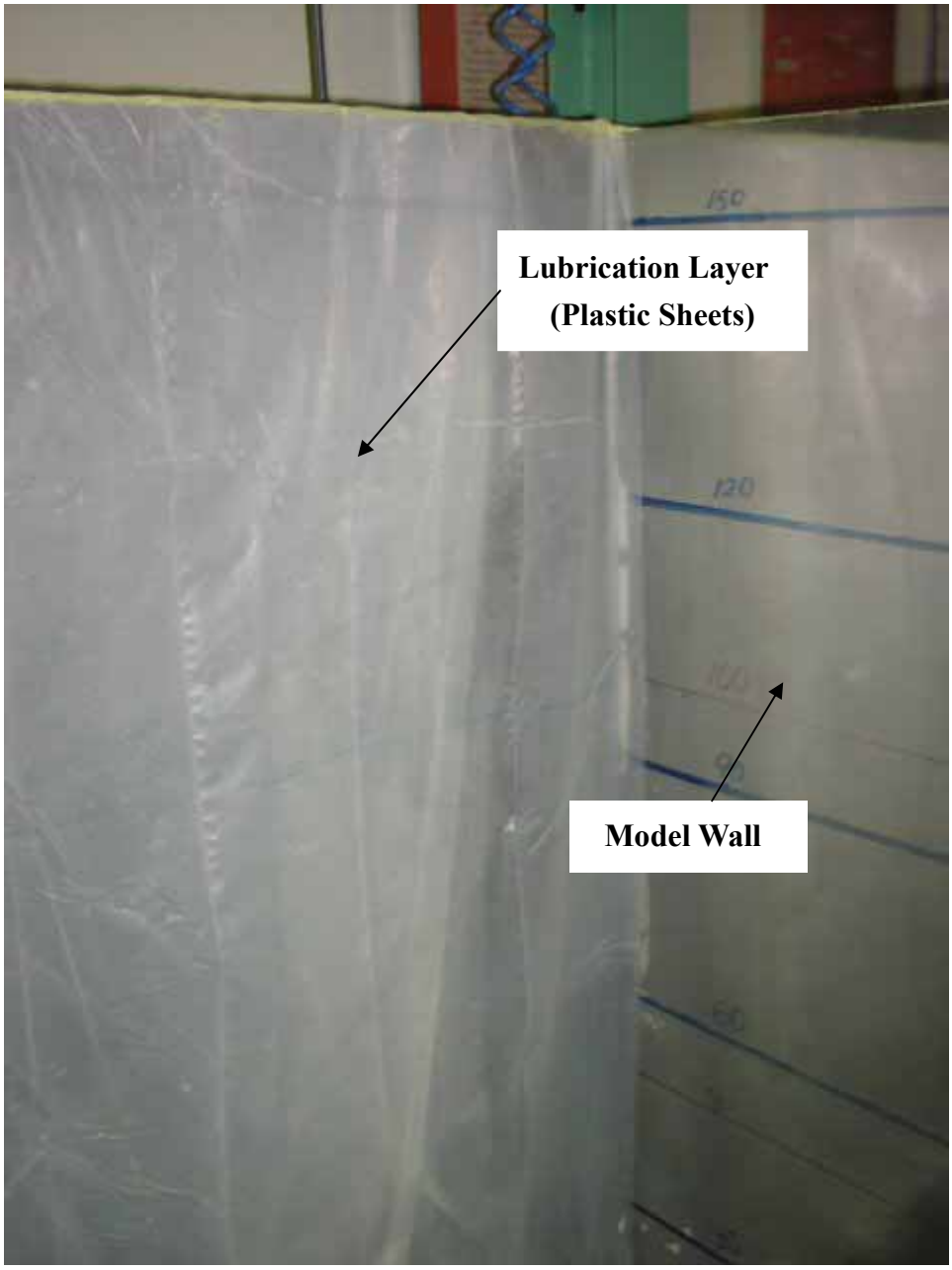

Fig. 5.22. Lubrication layer hung on the side wall

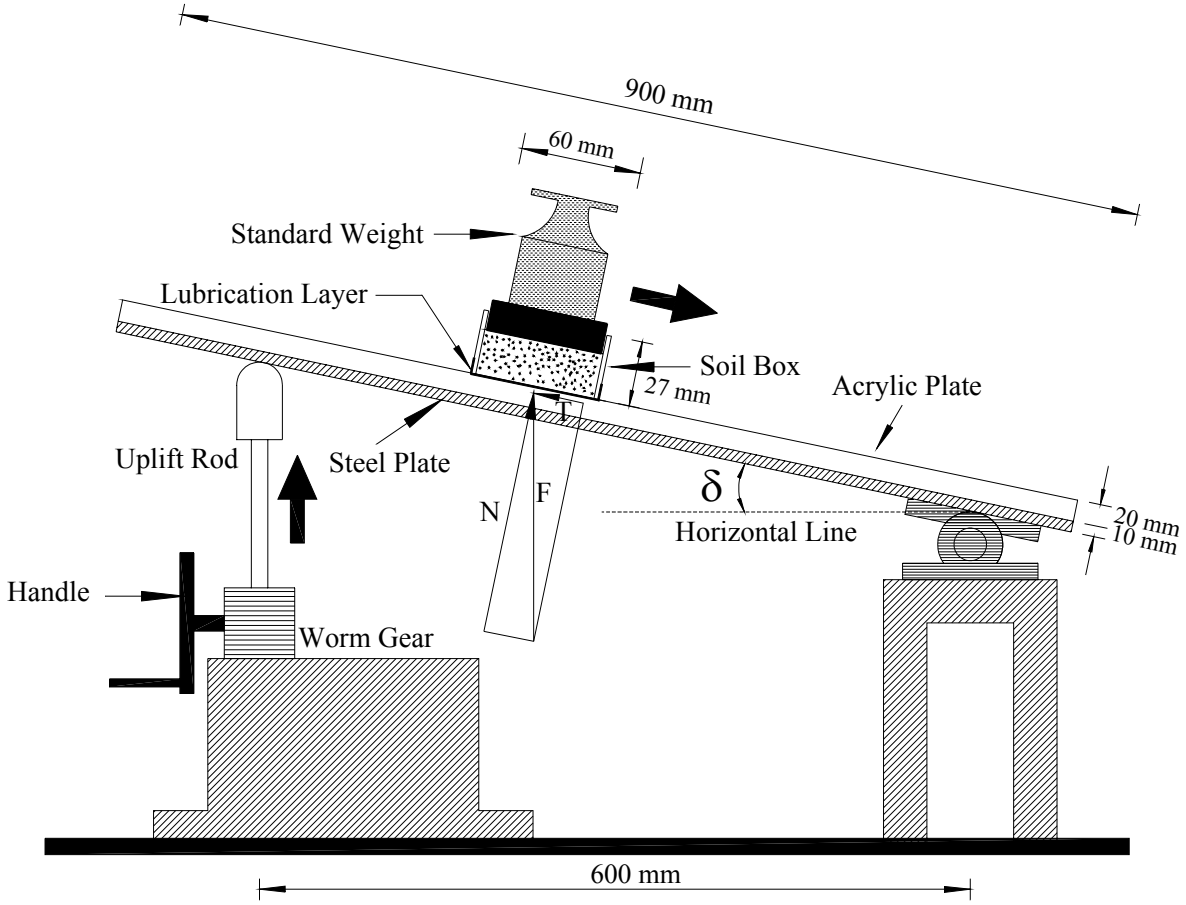

Fig. 5.23. Schematic diagram of sliding block test (after Fang et al., 2004)

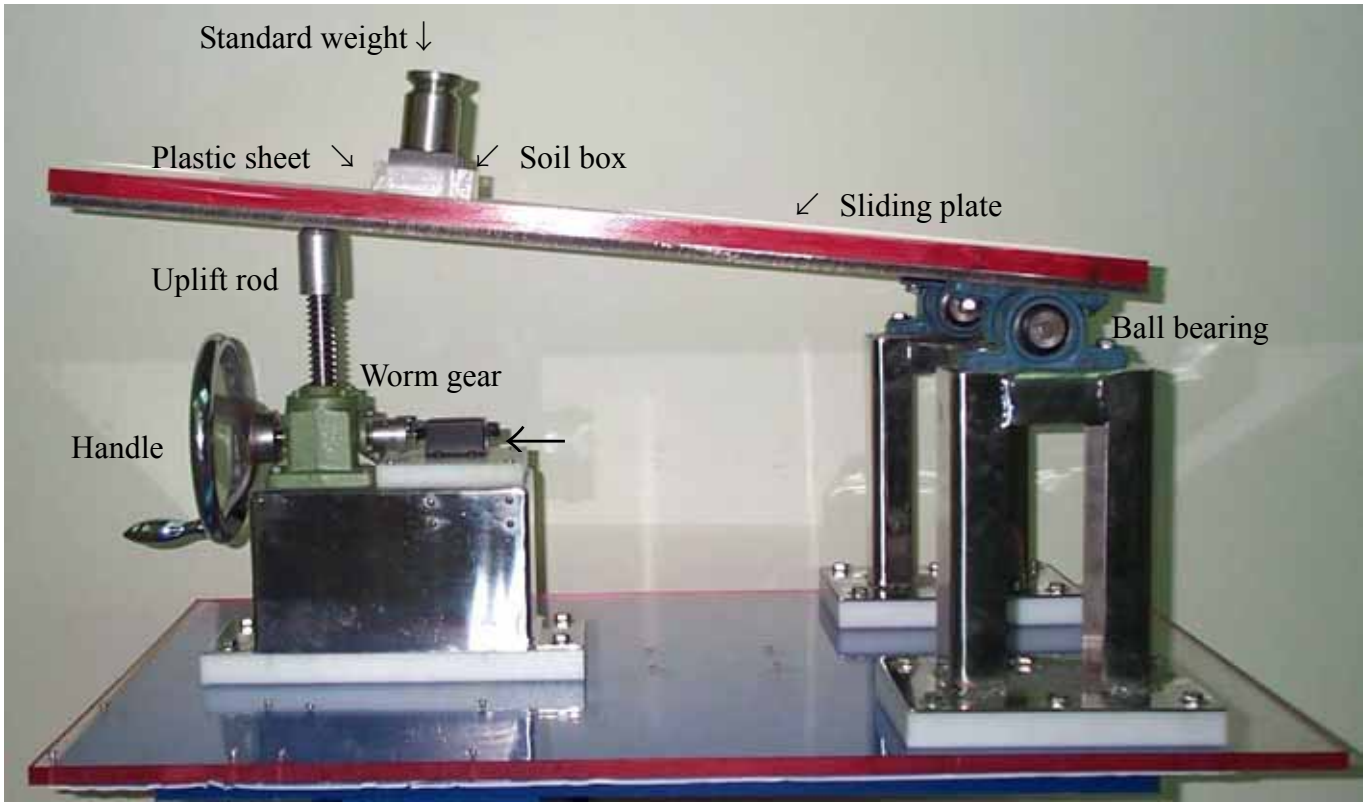

Fig. 5.24. Sliding block test apparatus (after Fang et al., 2004)

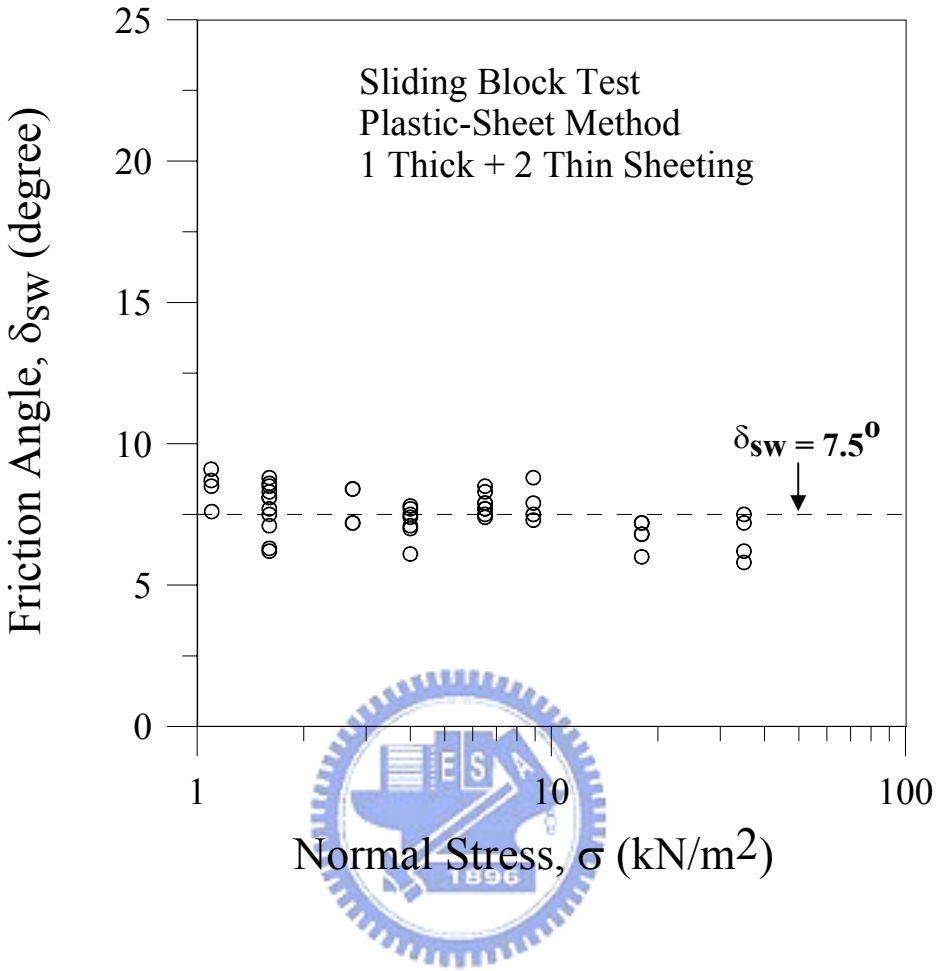

Fig. 5.25. Variation of interface angle with normal stress (after Fang et al., 2004)

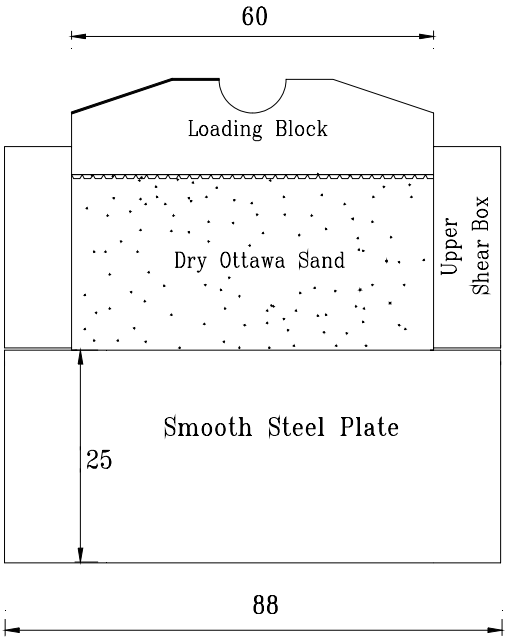

Unit : mm

(a)

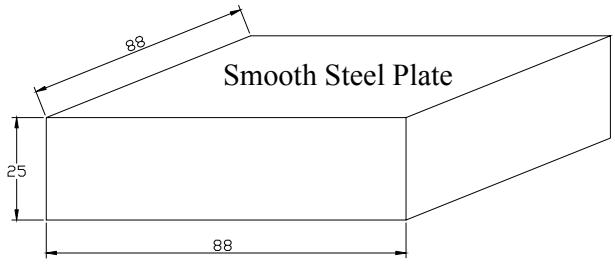

Unit : mm

(b) Smooth Steel Plate

Fig.5.26 Direct Shear Test Arrangement to Determinate Wall Friction Angle

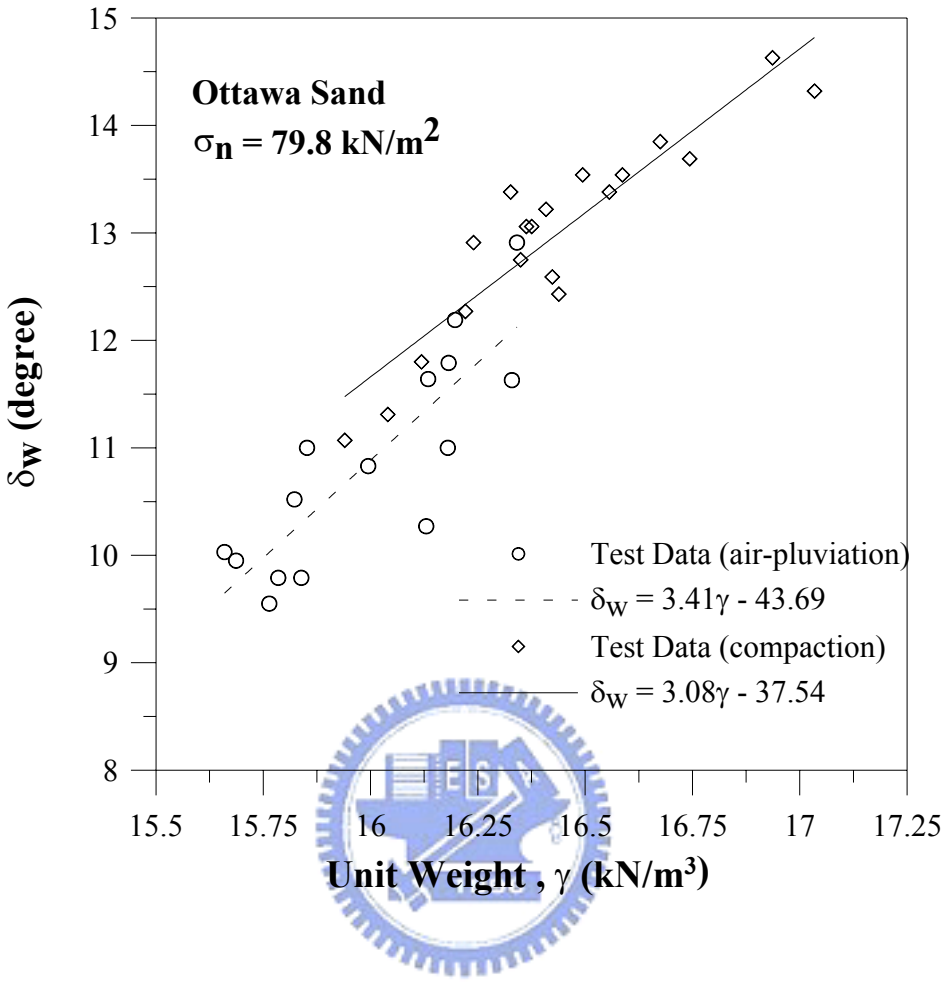

Fig. 5.27. Relationship between unit weight γ and wall friction angle δ_w (after Ho, 1999)

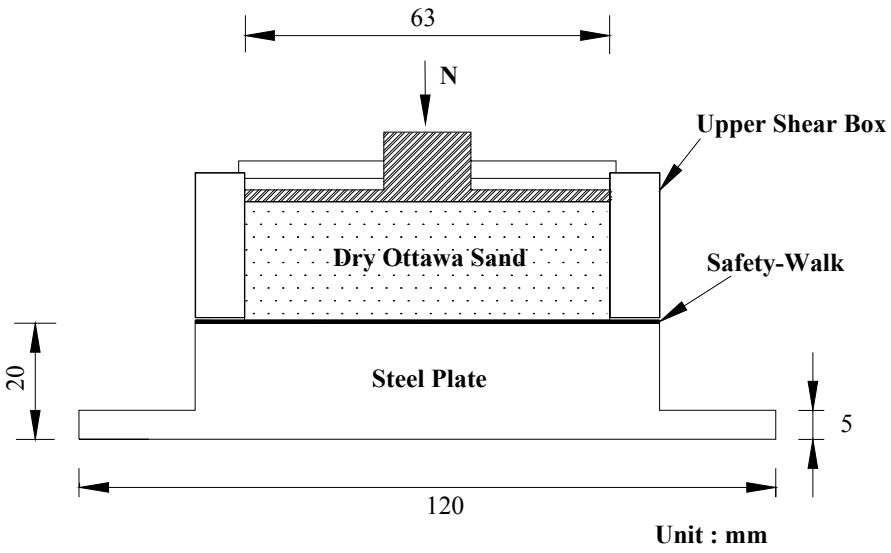

(a)

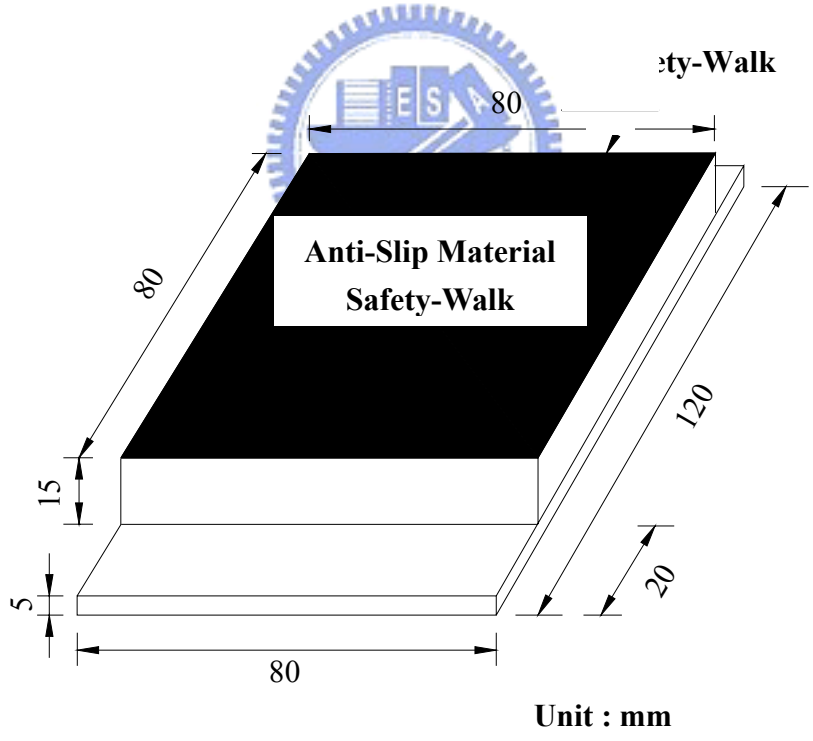

(b)

Fig. 5.28. Direct shear test arrangement to determine interface friction angle

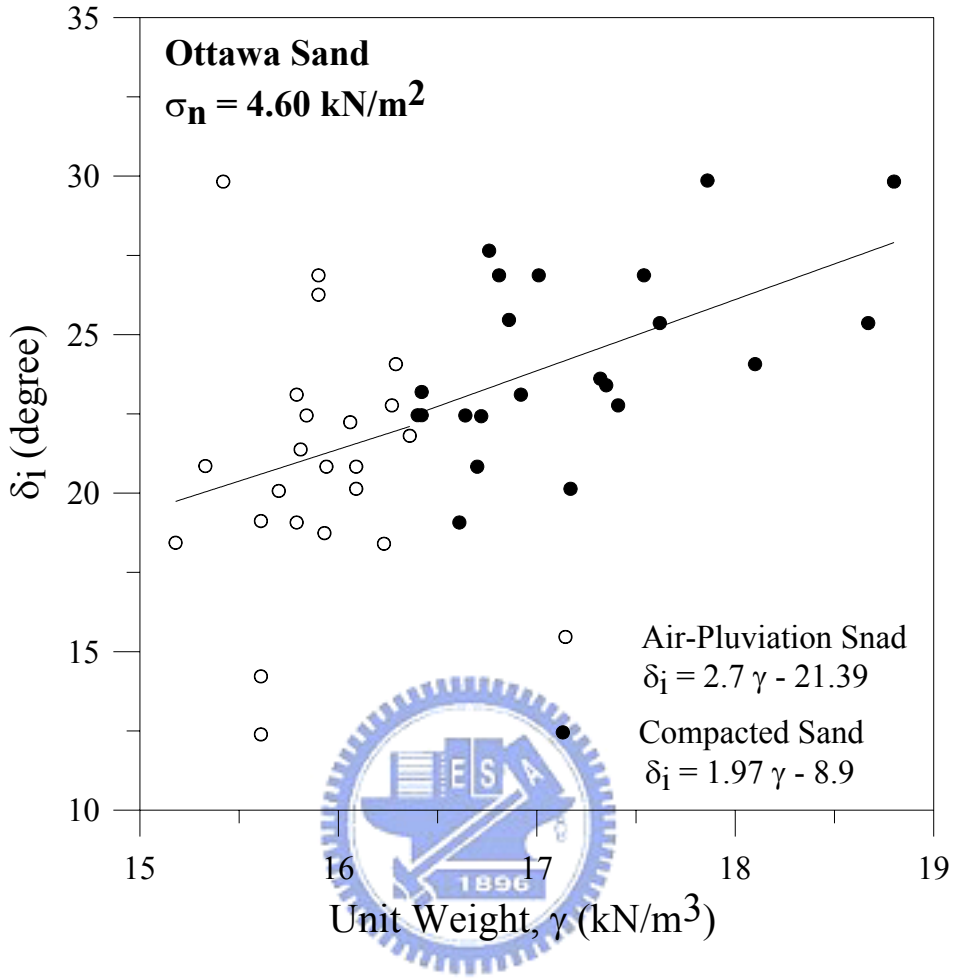

Fig. 5.29 Relationship between unit weight γ and interface plate friction angle δ_i

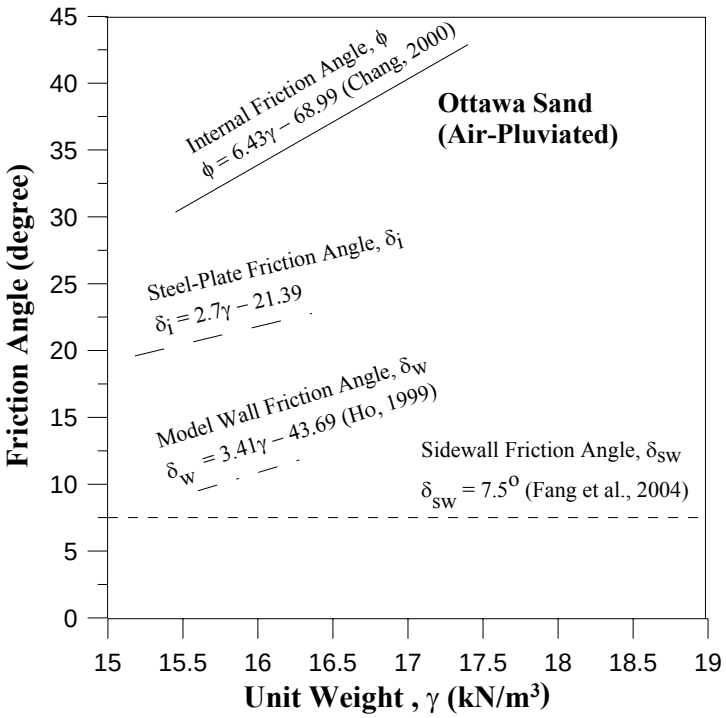

(a) Air-Pluviated Sand

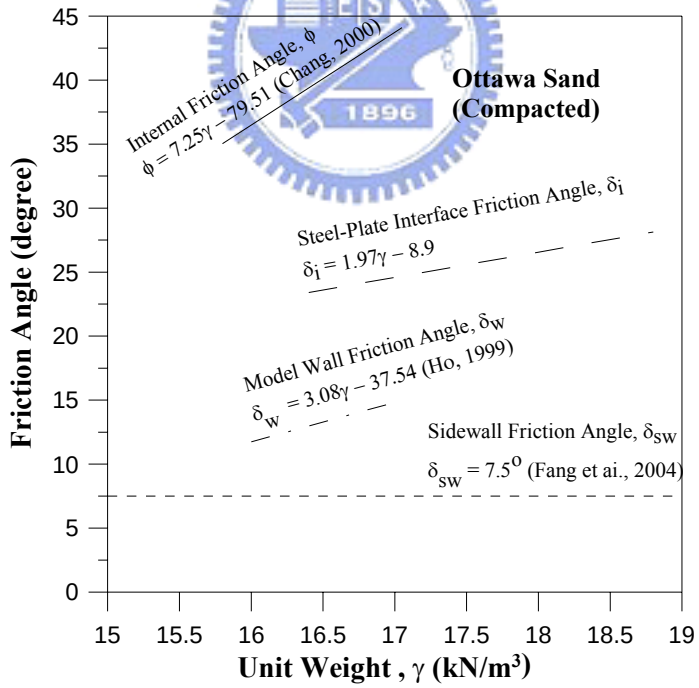

(b) Compacted Sand

Fig. 5.30. Relationship between unit weight γ and different friction angles